Vol 446|22 March 2007|doi:10.1038/nature05625

LETTERS

Peptide bond formation destabilizes Shine–Dalgarno interaction on the ribosome

Sotaro Uemura[1], Magdalena Dorywalska[2], Tae-Hee Lee[1], Harold D. Kim[1], Joseph D. Puglisi[2] & Steven Chu[1,3,4]

The ribosome is a molecular machine that translates the genetic code contained in the messenger RNA into an amino acid sequence through repetitive cycles of transfer RNA selection, peptide bond formation and translocation[1–3]. Here we demonstrate an optical tweezer assay to measure the rupture force between a single ribosome complex and mRNA. The rupture force was compared between ribosome complexes assembled on an mRNA with and without a strong Shine–Dalgarno (SD) sequence—a sequence found just upstream of the coding region of bacterial mRNAs, involved in translation initiation[4,5]. The removal of the SD sequence significantly reduced the rupture force in complexes carrying an aminoacyl tRNA, Phe-tRNA^{Phe}, in the A site, indicating that the SD interactions contribute significantly to the stability of the ribosomal complex on the mRNA before peptide bond formation. In contrast, the presence of a peptidyl tRNA analogue, N-acetyl-Phe-tRNA^{Phe}, in the A site, which mimicked the post-peptidyl transfer state, weakened the rupture force as compared to the complex with Phe-tRNA^{Phe}, and the resultant force was the same for both the SD-containing and SD-deficient mRNAs. These results suggest that formation of the first peptide bond destabilizes the SD interaction, resulting in the weakening of the force with which the ribosome grips an mRNA. This might be an important requirement to facilitate movement of the ribosome along mRNA during the first translocation step.

The ribosome is a complex catalytic machine, composed of more than 50 different proteins and three RNA chains, that performs protein synthesis. The 30S small subunit provides a framework on which tRNAs can accurately pair with the mRNA codons, whereas the 50S large subunit catalyses the formation of peptide bonds[1–3]. Structural and biochemical data have revealed a network of contacts between tRNAs bound to adjacent codons in the peptidyl- and aminoacyl-tRNA sites (P and A sites) and both the 30S and 50S subunits[6–9]. Ribosome–tRNA–mRNA interactions are required for the maintenance and regulation of the ribosomal complex stability during all stages of translation, yet processive translocation requires relaxation of the interactions for movement of tRNA–codon complexes with respect to the ribosome. Initial positioning of the ribosome on mRNA involves the recognition of a purine-rich sequence, known as the Shine–Dalgarno (SD) sequence, located upstream of the AUG initiation codon on the mRNA and complementary to the 3′ end of the 16S rRNA[4,5].

Although the detailed interactions between the translation components have been revealed by extensive structural and biochemical studies, it is not known how the precise regulation of macromolecular movements required at each stage of translation is achieved. It remains unclear what signal induces the substantial and well-tuned macromolecular forces that the ribosome must generate following every peptide bond formation to trigger the progress of its 25-kDa tRNA substrates through the intersubunit active sites along with its own precise directional movement by one codon down the mRNA.

Here, using optical tweezers, we measure directly the forces exerted between the ribosome and mRNA in the context of various tRNAs before and after peptide bond formation. Ribosome complexes were assembled on a 57 nucleotide mRNA derived from the T4 gene 32

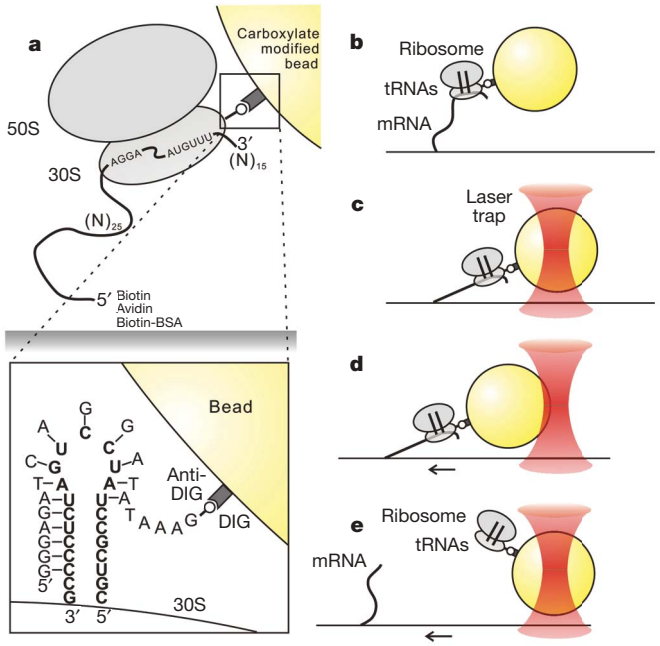

Figure 1 | Experimental design for rupture force measurements on the ribosome. a, The molecular attachments within the mRNA–ribosome–bead complex. Ribosomal particles were assembled on a short mRNA tethered to the surface via biotin–streptavidin linkage. A digoxigenin-modified oligonucleotide was designed to hybridize to an rRNA loop extension on the small ribosomal subunit (see magnified view at bottom). A bead coated with anti-digoxigenin antibody was conjugated to the oligonucleotide and used for optical trapping of the ribosomal complex. The sequence 'AGGA' on the mRNA designates the strong SD region, 'AUGUUU' indicates the first two codons of the mRNA, $(N)_{25}$ and $(N)_{15}$ specify the number of residues in the upstream and downstream regions, respectively, and 'Biotin Avidin Biotin-BSA' indicates the details of mRNA attachment to the surface. **b**, The tethered ribosome–bead complex fluctuates around the point of surface attachment. The two parallel lines within the ribosome signify the two tRNAs bound at the A and P sites. **c**, Optical tweezers are used to trap the bead. **d**, As the stage with the attached ribosome–bead complex is moved in one direction, the force exerted on the complex increases and the bead becomes displaced. **e**, Eventually the external force becomes sufficient to rupture the complex, and the bead returns to the trap centre position.

[1]Department of Physics, [2]Department of Structural Biology, Stanford University, Stanford, California 94305, USA. [3]Lawrence Berkeley National Laboratory, Berkeley, California 94720, USA. [4]Departments of Physics, Molecular and Cellular Biology, University of California, Berkeley, California 94720, USA.

mRNA, containing a natural SD sequence and a 5′ biotin modification to tether the complex to streptavidin-derivatized quartz surfaces. For optical trapping, 1-μm-diameter carboxylate-modified beads coated with anti-digoxigenin antibody were bound to a digoxigenin-modified DNA oligonucleotide designed to hybridize to an extension genetically engineered into helix 44 of the *Escherichia coli* 16S rRNA[10] (Fig. 1a, b). A single bead bound to a single ribosome complex—as verified by single step fluorescence photobleaching of Cy3-labelled tRNA in the P site (Supplementary Fig. 1a, b)—was tethered to the surface via mRNA and trapped with optical tweezers (Fig. 1c). The piezo stage was moved at a constant velocity ($\sim$100 nm s^{-1}) in one direction followed by a movement of the bead (Fig. 1d) until the external force exerted on the ribosome resulted in a rupture event and a rapid return of the bead to the trap centre position (Fig. 1e). External force was applied at a relatively fast rate to minimize possible dissociation of the ribosome complex during the measurement (Supplementary Methods).

Several examples of rupture force events recorded for tethered mRNA–ribosome–bead complexes are shown in Fig. 2a. Rupture events probably result from ribosome dissociation from the mRNA, as no rupture events were observed in the following two sets of control experiments: in one set of experiments, the ribosomes were crosslinked directly to a cysteine-reactive surface instead of being tethered via mRNA (Fig. 2b); in the other, the ribosome–mRNA complex was replaced by a surface-attached biotinylated RNA oligonucleotide of the same sequence as the rRNA extension complementary to the DNA oligonucleotide–bead conjugate (Fig. 2c). These results demonstrate that the ribosome–oligonucleotide interactions that anchor the bead onto the ribosome are sufficiently strong for force measurements within the required range. In addition, post-rupture colocalization of the bead and the ribosome complex with fluorescent tetramethylrhodamine-labelled[11] tRNA in the P site suggests that the rupture involves disruption of tRNA–mRNA interactions, because after the rupture event the mRNA is attached to the surface while the tRNA remains on the bead-associated ribosome (data not shown). This provided further proof that the observed rupture does not occur at the ribosome–oligonucleotide–bead linkage.

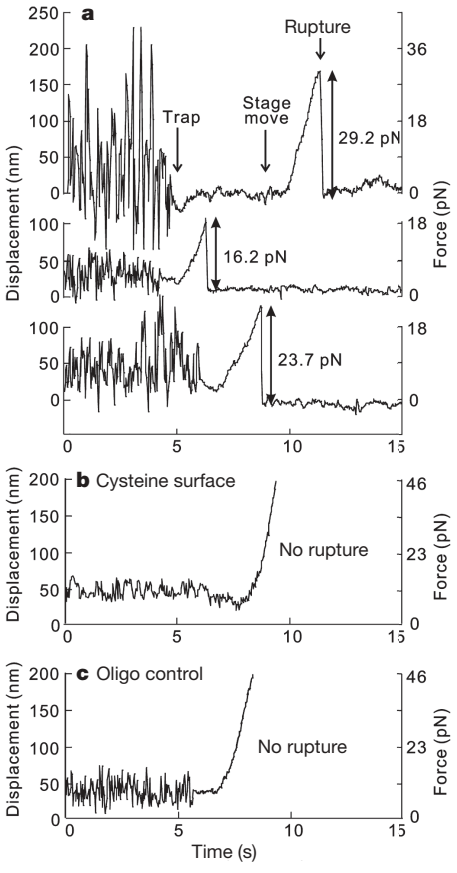

Figure 2 | Examples of displacement–time traces, showing the behaviour of the bead. **a**, The position of tethered beads fluctuates around the tether centre. Once the bead is trapped by the optical tweezers, its fluctuations become suppressed as indicated. As the bead starts to follow the stage movement, the force exerted on the complex increases. When the ribosome complex ruptures, the bead returns to the trapping centre. **b**, Control measurement for ribosomes covalently crosslinked to a cysteine-reactive surface. No rupture events were observed within our measurement range. **c**, Control measurement for a biotinylated RNA oligonucleotide designed to mimic the extension in the 16S rRNA. The RNA oligonucleotide was attached to a streptavidin-derivatized surface and hybridized with the DNA oligonucleotide–bead conjugate. No rupture events were observed.

Binding of tRNAs to the ribosome stabilizes ribosome–mRNA interactions. The rupture force distribution for a ribosome–mRNA complex in the absence of tRNAs showed a single peak at 10.6 pN (Fig. 3a). The addition of non-acylated initiator tRNA^{fMet} to the P site strengthened the ribosome–mRNA interactions roughly by 5 pN, increasing the rupture force to 15.2 pN (Fig. 3b). Subsequent addition of Phe-tRNA^{Phe} to the A site resulted in further stabilization of the complex by another 10 pN, giving a single peak distribution centred at 26.5 pN (Fig. 3c). In all experiments, the tRNA occupancy of each ribosome complex was verified just before the force measurement using fluorescence resonance energy transfer (FRET). For this purpose, tRNA^{fMet} in the P site was labelled with Cy3, Phe-tRNA^{Phe} in the A site was labelled with Cy5, and fluorescence of both dyes was monitored at 532 nm excitation following methods described previously[12] (Supplementary Fig. 1). Only complexes showing FRET owing to the presence of both tRNAs were included in further force measurement analysis, so that the final force population distributions are representative of ribosomal complexes with both A and P sites occupied (Fig. 3c–f, i, j). The multiple interactions between P-site and A-site tRNAs and both the large and small ribosomal subunits[6,7] probably contribute to the stabilization of the ribosomal complex on the mRNA and explain the large rupture force increase upon the addition of tRNAs.

The nature of the aminoacyl group on A-site tRNA strongly affects ribosome–mRNA rupture forces. Binding of the peptidyl-tRNA analogue N-acetyl-Phe-tRNA^{Phe} to the A site, which mimics the post-peptidyl transfer state, resulted in a significant reduction of the rupture force to 12.7 pN (Fig. 3d), suggesting that the interactions between the ribosome and mRNA are weakened after peptide bond formation. The lower affinity of the peptidyl-tRNA in the A site[13] might also contribute to the decrease in rupture force. Complexes prepared with fMet-tRNA^{fMet} in the P site and Phe-tRNA^{Phe} in the A site, allowing for efficient formation of a ribosome-catalysed peptide bond, showed a weak rupture force centred at 11.4 pN, with only a minor peak at 24.8 pN most probably representative of a small subpopulation (14.3%) of either inactive ribosomes and/or ribosomes where the P-site tRNA has become deacylated (Fig. 3e). This provides further evidence that the presence of the peptidyl-tRNA moiety in the A site results in the destabilization of ribosome–mRNA interactions. In addition, the stability of the ribosome on mRNA is not affected by the equilibrium between the classical and hybrid tRNA states. In related work, we have observed that the post-peptide bond mimic (tRNA^{fMet} in the P site and N-acetyl-Phe-tRNA^{Phe} in the A site) results in rapid classical–hybrid state fluctuations at 5 mM Mg^{2+} (with the relative occupancy of classical and hybrid states of 3:2), while the tRNAs remain predominantly in the classical configuration at 15 mM Mg^{2+} (H.D.K. *et al.*, manuscript in preparation). No significant difference was observed in the rupture force distributions of the post-peptidyl transfer complex in 5 mM Mg^{2+} and 15 mM Mg^{2+} buffers (compare Fig. 3d and f). Whereas different Mg^{2+} concentrations can affect tRNA–ribosome complex stability[13], the timescale of

tRNA dissociation is much greater than the time it took to complete the force measurements. The observed lack of strong Mg^{2+} dependence to the measured forces indicates that we are monitoring rupture of mRNA–ribosome base pairings, which are not strongly Mg^{2+} dependent.

The SD interaction directly increases the binding affinity of the ribosome for mRNA and influences tRNA–mRNA translocation[5,14]. To test the contribution of the SD interaction to complex stability, rupture measurements were performed on ribosomal complexes assembled on an mRNA where the SD interaction had been significantly weakened by modifying the sequence from AGGA to ACCA[14]. In the absence of tRNAs, no tethered beads were observed, indicating that the complexes without the SD region were too unstable for a force measurement (Fig. 3g). The addition of $tRNA^{fMet}$ to the P site stabilized the complexes by almost 5 pN, which is similar to the stabilization observed for the SD-containing complexes, allowing for a rupture force measurement of 4.8 pN (Fig. 3h). Further addition of Phe-$tRNA^{Phe}$ to the A site increased the rupture force to 14.8 pN (Fig. 3i), a 10 pN increase again similar to that observed for the SD-containing complexes. Upon binding of N-acetyl-Phe-$tRNA^{Phe}$ to the complexes without the SD sequence, a rupture force of 12.1 pN was measured (Fig. 3j), slightly reduced in comparison to the force observed for Phe-$tRNA^{Phe}$ complexes (Fig. 3i). This final post-peptidyl transfer rupture force was essentially the same for the SD-containing and SD-lacking complexes (compare Fig. 3d and j), which raises the possibility that peptide bond formation results in destabilization of SD interactions between the mRNA and the small ribosomal subunit.

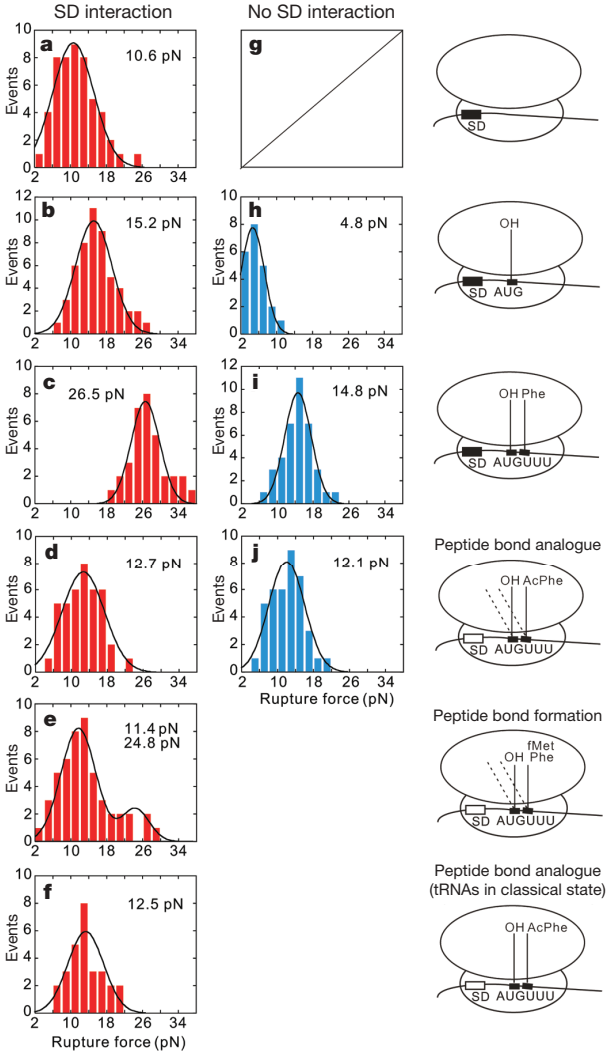

Figure 3 | Rupture force distributions for ribosome complexes assembled on mRNAs containing (left panels) or lacking (middle panels) the SD sequence. The numbers above each histogram are the force values determined for each complex. All complexes were assembled in 5 mM Mg^{2+} unless indicated otherwise. **a**, **g**, Ribosome–mRNA complex without tRNAs. No tethered beads were observed in the absence of the SD sequence (**g**), indicating that the complex was too unstable for a force measurement under these conditions. **b**, **h**, Ribosome–mRNA complex carrying deacylated $tRNA^{fMet}$ in the P site. **c**, **i**, Ribosome–mRNA complex with $tRNA^{fMet}$ in the P site and Phe-$tRNA^{Phe}$ in the A site. **d**, **j**, Ribosome–mRNA complex with $tRNA^{fMet}$ in the P site and N-acetyl-Phe-$tRNA^{Phe}$ in the A site. **e**, Ribosome–mRNA complex after ribosome-catalysed peptide bond formation. The complex was assembled with fMet-$tRNA^{fMet}$ in the P site and Phe-$tRNA^{Phe}$ in the A site, and incubated for 20 min to allow for peptidyl transfer. **f**, Ribosome–mRNA complex with $tRNA^{fMet}$ in the P site and N-acetyl-Phe-$tRNA^{Phe}$ in the A site in 15 mM Mg^{2+}. The diagrams on the right show the composition of the complexes containing the SD sequence: strong SD interactions are indicated by black boxes, while destabilized SD interactions are shown as white boxes.

Although the exact rupture pathway cannot be determined for the different ribosomal complexes, Cy3 and Cy5 fluorescence analysis verified the initial tRNA occupancy on the ribosomes. Owing to the rapid photobleaching of Cy3 in the presence of high intensity optical trapping light, we could not confirm tRNA occupancy after the force measurement using the same dye pair. Separate experiments using tetramethylrhodamine-labelled tRNA to demonstrate post-rupture colocalization of the ribosome complex and the bead suggest that the rupture occurs through the disruption of interactions between the 30S–tRNA complexes and the mRNA, as the 30S subunit and at least one bound tRNA remain attached to the bead, while the mRNA stays anchored on the surface via the strong biotin–streptavidin link. As both the initial and the final ligand-bound states are comparable for the different ribosome complexes, the rupture pathways are presumed to be similar and are unlikely to involve an intermediate spontaneous translocation step (known to occur in the absence of EF-G at a very slow rate[15]) or spontaneous dissociation of the entire ribosomal complex on the timescale of the force measurement experiment.

Our results provide direct evidence for coupling of the 50S peptidyl transferase centre and the 30S subunit. Precisely how the formation of a peptide bond on the 50S portion of the ribosome leads to the weakening of the mRNA contacts with the 30S subunit needed for processive translation is yet to be determined. Previous studies have demonstrated that the ribosome can sense the chemical nature of its ligand in the A site: peptidyl-tRNA shows much lower binding affinity than aminoacyl-tRNA[13], while deacylation of the A-site bound tRNA can affect the accuracy of translocation along mRNA[14]. The distinct interactions of aminoacyl-tRNA versus peptidyl-tRNA moieties at the peptidyl transferase centre after peptide bond formation might induce conformational changes within the 50S subunit, which could be further propagated through the subunit interface towards the anti-SD region of the 30S subunit, possibly via a relative movement of the two subunits[16], resulting in the destabilization of SD interactions between the 30S subunit and mRNA, and facilitating the first translocation step. A mechanistic explanation of this allosteric communication requires further investigation.

Received 29 July 2006; accepted 26 January 2007.

1. Noller, H. F. Structure of ribosomal RNA. *Annu. Rev. Biochem.* **53**, 119–162 (1984).
2. Wintermeyer, W. *et al.* Mechanisms of elongation on the ribosome: dynamics of a macromolecular machine. *Biochem. Soc. Trans.* **32**, 733–737 (2004).
3. Green, R. & Noller, H. F. Ribosomes and translation. *Annu. Rev. Biochem.* **66**, 679–716 (1997).
4. Shine, J. & Dalgarno, L. The 3′-terminal sequence of *Escherichia coli* 16S ribosomal RNA: complementarity to nonsense triplets and ribosome binding sites. *Proc. Natl Acad. Sci. USA* **71**, 1342–1346 (1974).

5. Calogero, R. A., Pon, C. L., Canonaco, M. A. & Gualerzi, C. O. Selection of the mRNA translation initiation region by *Escherichia coli* ribosomes. *Proc. Natl Acad. Sci. USA* **85,** 6427–6431 (1988).
6. Yusupov, M. M. *et al.* Crystal structure of the ribosome at 5.5 Å resolution. *Science* **292,** 883–896 (2001).
7. Yusupova, G. Z., Yusupov, M. M., Cate, J. H. D. & Noller, H. F. The path of messenger RNA through the ribosome. *Cell* **106,** 233–241 (2001).
8. Moazed, D. & Noller, H. F. Interaction of tRNA with 23S rRNA in the ribosomal A, P, and E sites. *Cell* **57,** 585–597 (1989).
9. Moazed, D. & Noller, H. F. Binding of tRNA to the ribosomal A and P sites protects two distinct sets of nucleotides in 16S rRNA. *J. Mol. Biol.* **211,** 135–145 (1990).
10. Dorywalska, M. *et al.* Site-specific labeling of the ribosome for single-molecule spectroscopy. *Nucleic Acids Res.* **33,** 182–189 (2005).
11. van Dijk, M. A., Kapitein, L. C., van Mameren, J., Schmidt, C. F. & Peterman, E. J. G. Combining optical trapping and single-molecule fluorescence spectroscopy: Enhanced photobleaching of fluorophores. *J. Phys. Chem. B* **108,** 6479–6484 (2004).
12. Blanchard, S. C., Kim, H. D., Gonzalez, R. L. Jr, Puglisi, J. D. & Chu, S. tRNA dynamics on the ribosome during translation. *Proc. Natl Acad. Sci. USA* **101,** 12893–12898 (2004).
13. Semenkov, Y. P., Rodnina, M. V. & Wintermeyer, W. Energetic contribution of tRNA hybrid state formation to translocation catalysis on the ribosome. *Nature Struct. Biol.* **7,** 1027–1031 (2000).
14. Fredrick, K. & Noller, H. F. Accurate translocation of mRNA by the ribosome requires a peptidyl group or its analog on the tRNA moving into the 30S P site. *Mol. Cell* **9,** 1125–1131 (2002).
15. Katunin, V. I., Savelsbergh, A., Rodnina, M. V. & Wintermeyer, W. Coupling of GTP hydrolysis by elongation factor G to translocation and factor recycling on the ribosome. *Biochemistry (Mosc.)* **41,** 12806–12812 (2002).
16. Frank, J. & Agrawal, R. K. A ratchet-like inter-subunit reorganization of the ribosome during translocation. *Nature* **406,** 318–322 (2000).

Supplementary Information is linked to the online version of the paper at www.nature.com/nature.

Acknowledgements We thank C. Squires for the SQ380 strain that was used to engineer the ribosomes. We are grateful to colleagues in the S. Chu and J. Puglisi groups at Stanford University for encouragement and discussions. S.U. is a recipient of JSPS Postdoctoral Fellowships for Research Abroad. M.D. was supported by the HHMI Predoctoral Fellowship. This work was funded by grants to J.D.P. from the NIH and the Packard Foundation, to S.C. from the NSF and NASA, and to J.D.P. and S.C. from the Packard Foundation.

Author Information Reprints and permissions information is available at www.nature.com/reprints. The authors declare no competing financial interests. Correspondence and requests for materials should be addressed to J.D.P. (puglisi@stanford.edu) or S.C. (schu@lbl.gov).